nature synthesis

Article

https://doi.org/10.1038/s44160-026-01127-z

Aziridination of inert alkanes via photo-mediated double hydrogen atom transfer

Received: 30 July 2025

Accepted: 3 July 2026

Published online: 30 July 2026

Check for updates

Ming-Shang Liu[1,5], Hwee Ting Ang[1,5], Qing-Yang Zhou[2], Chu Wang[1], Xiao-Ye Yu[1], Jun-Li Ao[1,3], Gan Wang[1], Zi-Hao Jiao[1], Kendall N. Houk[2] ✉ & Jie Wu[1,4] ✉

The direct functionalization of inert alkanes is a long-standing challenge in synthetic chemistry owing to the high bond dissociation energy of C(sp^3)–H bonds. Hydrogen atom transfer (HAT) has emerged as a powerful strategy for monofunctionalization, while the development of methods enabling vicinal double functionalization of alkanes remains limited and typically relies on a monofunctionalization–β-elimination–difunctionalization cascade. Here we report the development of a double-HAT process, leveraging the distinctive reactivity of photo-generated triplet sulfonyl nitrenes under visible-light irradiation, to directly transform inert alkanes into aziridines. This approach streamlines the synthesis of diverse aziridines from readily available alkanes, with large-scale synthesis assisted by a high-speed circulation flow platform. Mechanistic insights, supported by both experimental and computational investigations, reveal the formation of an olefin intermediate through a double-HAT process, with the in situ-generated triplet sulfonyl nitrenes and iodosobenzene playing critical roles in the reaction pathway.

Alkanes, though abundant and inexpensive feedstocks, are underutilized in organic synthesis owing to their inert C–H bonds, which are challenging to activate because of the high bond dissociation energies. Direct functionalization of these C–H bonds is critical for advancing modern synthetic chemistry, offering an efficient, atom- and step-economical approach to transform inert alkanes into complex and value-added products[1]. Among various strategies, hydrogen atom transfer (HAT) catalysis, particularly photo-HAT, has emerged as a powerful tool, enabling the direct activation of C–H bonds into reactive carbon radicals under mild conditions without necessitating pre-functionalization or directing groups[2,3]. Despite its broad utility and potential, current HAT methodologies primarily focus on single C–H bond functionalization (Fig. 1a), leaving the double functionalization of adjacent aliphatic C–H bonds largely unexplored. Existing strategies for double C–H functionalization typically rely on a sequential HAT–monofunctionalization–β-elimination–difunctionalization cascade, requiring alkane substrates with neighbouring heteroatoms or activating groups[4–13] (Fig. 1b). In addition, sequential HAT for alkane-to-alkene conversion with unactivated alkanes[14–19] often necessitates multiple catalysts and steps. While double HAT using benzyne-mediated desaturation of alkanes to alkenes through the concurrent removal of two vicinal hydrogen atoms shows promise, its reliance on complex intermediates hampers its practical applicability[20] (Fig. 1c). Therefore, developing practical methods for double HAT of abundant alkane feedstocks for dual C–H difunctionalization remains a compelling challenge and an exciting opportunity for innovation.

[1]Department of Chemistry, National University of Singapore, Singapore, Singapore. [2]Department of Chemistry and Biochemistry, University of California, Los Angeles, Los Angeles, CA, USA. [3]State Key Laboratory of Functions and Applications of Medicinal Plants and School of Pharmacy, Guizhou Medical University, Guiyang, China. [4]National University of Singapore (Suzhou) Research Institute, Suzhou, People's Republic of China. [5]These authors contributed equally: Ming-Shang Liu, Hwee Ting Ang. ✉e-mail: houk@chem.ucla.edu; chmjie@nus.edu.sg

https://doi.org/10.1038/s44160-026-01127-z

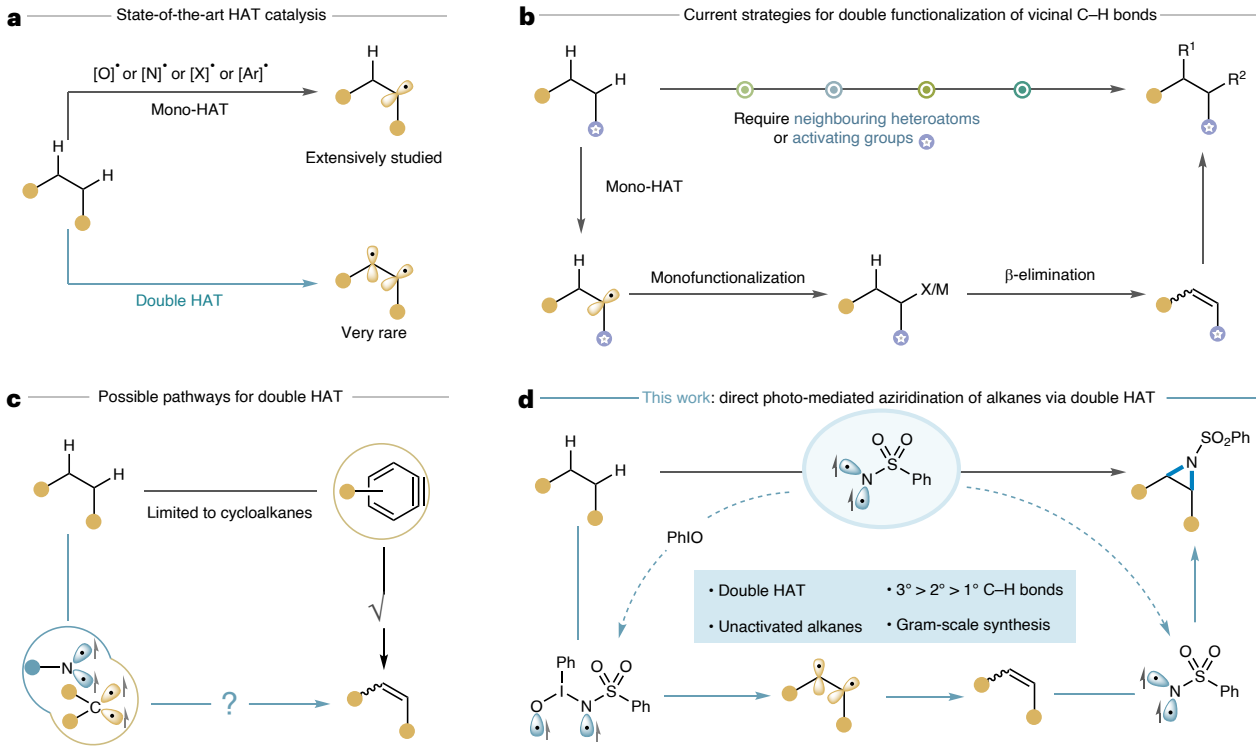

Fig. 1 | Aziridination of unactivated alkanes through a double-HAT process. a, State-of-the-art HAT catalysis. **b**, Current strategies for double functionalization of vicinal C–H bonds. **c**, Possible pathways for double HAT. **d**, This study: direct aziridination of alkanes using triplet sulfonyl nitrene intermediates.

Table 1 | Reaction optimization

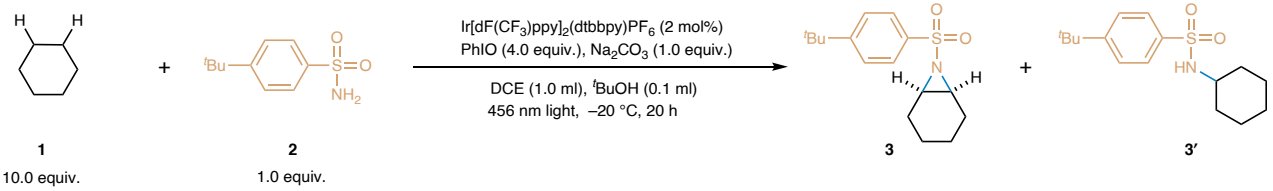

Entry	Variation from 'standard conditions'	3[a]	3′[a]	Entry	Variation from 'standard conditions'	3[a]	3′[a]
1	None	64% (60%)[b]	2%	6	PhIO (3.0 equiv.)	58%	7%
2	No Na_2CO_3	51%	3%	7	$PhI(OAc)_2$ instead of PhIO	8%	4%
3	No [Ir] catalyst	28%	Trace	8	0 °C	52%	3%
4	No light	ND	ND	9	*p*-^{t}Bu-C_6H_4-SO_2N_3, no PhIO	Trace	6%
5	PhIO (2.0 equiv.)	39%	8%	10	*p*-^{t}Bu-C_6H_4-SO_2N_3, PhIO (2.0 equiv.)	8%	3%

Standard conditions: **1** (10.0 equiv.), **2** (0.10 mmol), Ir[dF(CF_3)ppy]$_2$(dtbbpy)PF_6 (2 mol%), PhIO (4.0 equiv.), Na_2CO_3 (1.0 equiv.), in DCE (1.0 ml) and ^{t}BuOH (0.1 ml) using 456 nm light (20 W), at −20 °C for 20 h under argon. [a]Yields were determined based on the analysis of crude ^{1}H NMR spectra using mesitylene as an internal standard. [b]Isolated yield of **3**. ND, not detected.

Nitrenes and carbenes have garnered attention for their utilization in facilitating diverse reactions owing to their distinctive reactivity profiles. While singlet nitrenes and carbenes typically engage in direct C–H insertion with alkanes, their triplet counterparts present an intriguing alternative owing to their diradical nature. The greater stability and lower energy of triplet nitrenes or carbenes may enable a double-HAT process for difunctionalization of abundant alkane feedstocks (Fig. 1c). Triplet nitrenes, in particular, stand out as feasible intermediates for this approach owing to their tunable reactivity and accessibility under mild conditions. Recent advances in photochemistry have enabled the generation of transient and highly reactive nitrene species from various precursors, including iminoiodinanes, azides and amide N–O compounds, without the need for transition-metal catalysts[21,22]. Among these precursors, sulfonyl iminoiodinanes are particularly compelling because they can be generated in situ from sulfonamides using hypervalent iodides and activated by visible light to yield free sulfonyl nitrenes[23]. These nitrenes, accessible in both singlet and triplet states, exhibit interconvertibility, enabling diverse transformations, including alkene aziridination[24], sulfimidations[25], C(sp^3)–H amination of cyclic ethers[26] and Pauson–Khand-type reactions[27]. However, achieving a double-HAT process poses a central challenge: mitigating competitive radical–radical coupling—a well-recognized termination

https://doi.org/10.1038/s44160-026-01127-z

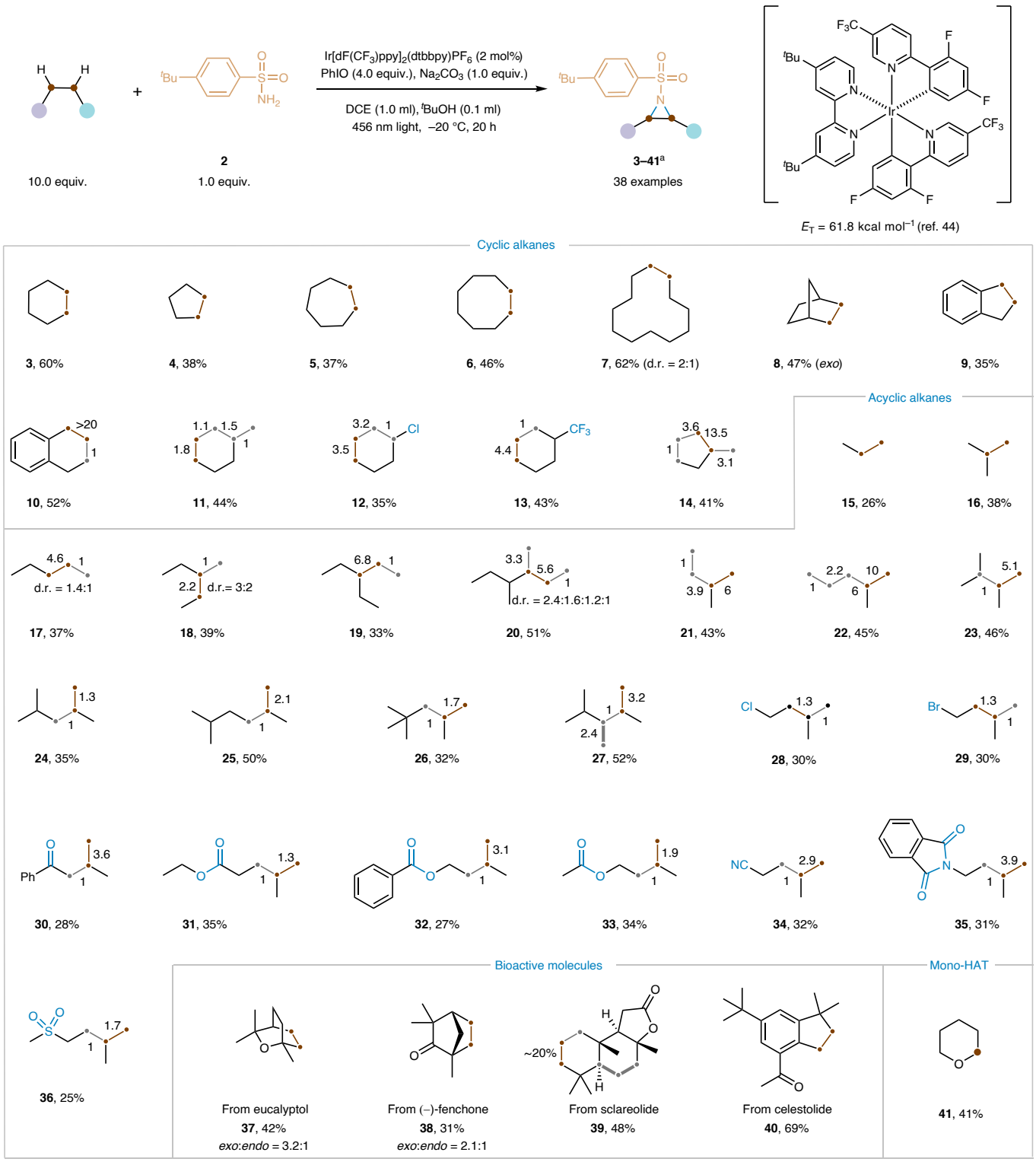

Fig. 2 | Reaction scope of hydrocarbons in aziridination. [a]Isolated overall yields of regio- and diastereoisomers. Isomer ratios were determined by the analysis of the crude ^{1}H NMR spectra. Numbers adjacent to each bond indicate the relative regioselectivity at that position. The starting materials are shown to illustrate site selectivity, and product structures are not depicted for clarity.

step in conventional radical processes—in favour of disproportionation resulting from an intermolecular head-to-tail HAT between radical species, where these competing pathways are strongly influenced by the spin-polarity and spatial orientation of the radicals[28].

We describe a double-HAT-enabled aziridination of unactivated alkanes under visible-light irradiation using in situ-generated sulfonyl iminoiodinanes, achieving synthetically useful yields. Aziridines, highly strained triangular nitrogen-containing heterocycles, are versatile synthetic intermediates en route to structurally complex molecules through ring-opening, expansion and rearrangement reactions[29–31]. While the aziridination of alkenes has been extensively explored using nitrenes (singlet or triplet), hydroxylamines or free amines[32–40], the synthesis of aziridines directly from unactivated alkanes remains underexplored. In this study, we overcome this challenge by generating

https://doi.org/10.1038/s44160-026-01127-z

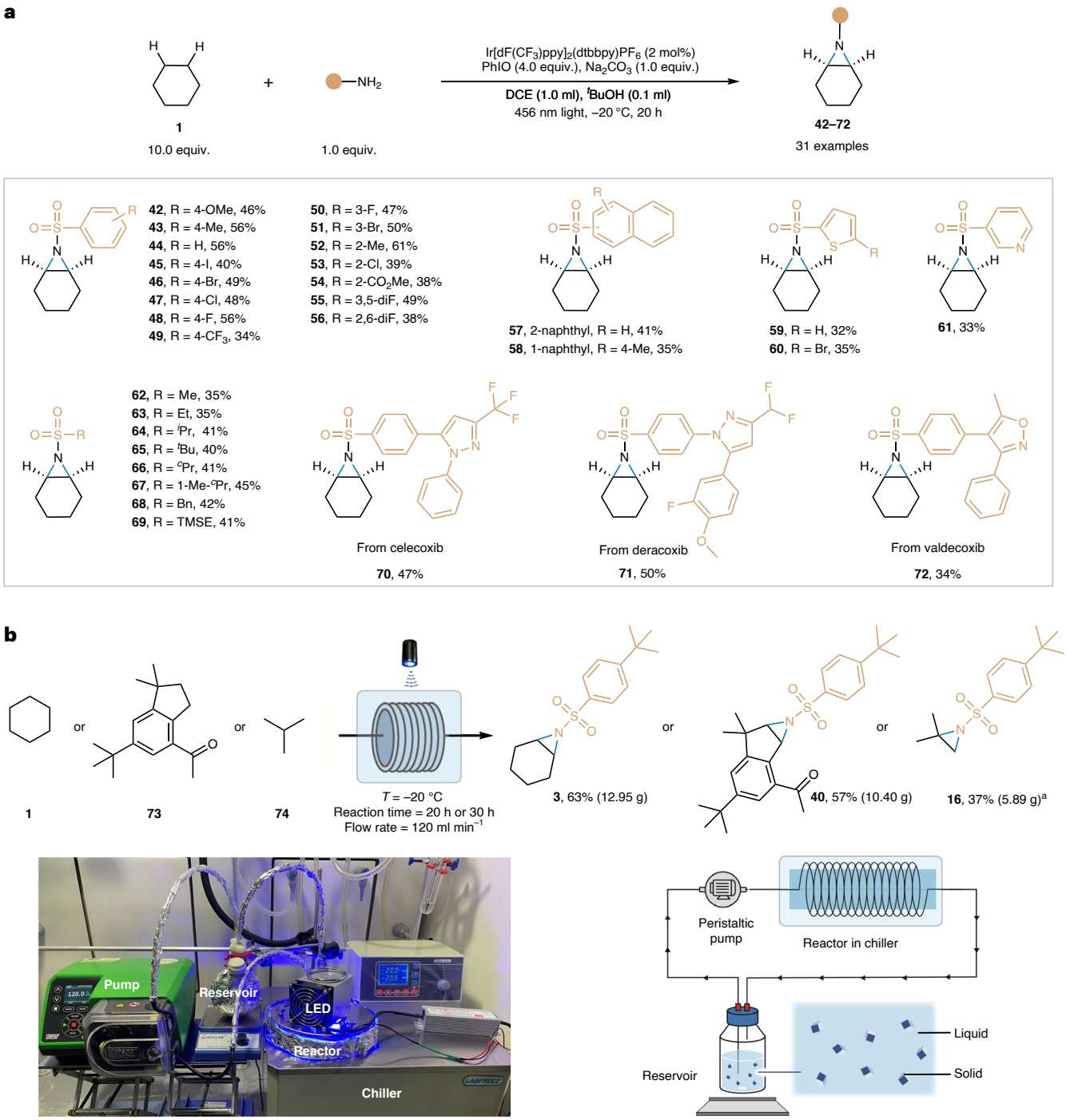

Fig. 3 | Reaction scope of sulfonamides and large-scale flow synthesis. **a**, Reaction scope of sulfonamides. **b**, Decagram-scale synthesis enabled by a high-speed circulation flow system. Isolated yields are reported. iPr, isopropyl; tBu, *tert*-butyl; cPr, cyclopropyl; TMSE, trimethylsilyl ethyl. [a]An additional pump (gas flow rate of 10 ml min^{-1}) was used to introduce isobutane gas into the system for the synthesis of **16** (Supplementary Fig. 43).

a triplet sulfonyl nitrene intermediate, which initiates the double HAT of adjacent aliphatic C–H bonds in the presence of iodosobenzene (PhIO) and serves as the nitrogen source for the subsequent aziridination (Fig. 1d). This approach not only expands the scope of double C–H functionalizations but also provides a practical method for synthesizing aziridines directly from alkanes.

Results and discussion

Reaction optimization

Our study commenced with cyclohexane **1** as a model alkane substrate to evaluate various nitrene precursors. Through extensive optimization, we identified that the combination of sulfonamide **2** and PhIO effectively generated aziridine **3** in good yield. The optimal reaction parameters were established as follows: using **2** as the limiting reagent, combined with **1** (10 equiv.), PhIO (4 equiv.), Na_2CO_3 (1 equiv.) and Ir[dF(CF_3)ppy]$_2$(dtbbpy)PF_6 (2 mol%) in a dichloroethane (DCE)/tBuOH cosolvent system, conducted at −20 °C under 456 nm light irradiation (20 W) for 20 h. Under these conditions, aziridine **3** was isolated in 60% yield, accompanied by a minor 2% yield of the C(sp^3)–H amination by-product **3′** (Table 1, entry 1). The omission of either Na_2CO_3 or the photocatalyst led to decreased yields of aziridine **3** (entries 2 and 3), while omitting light completely suppressed the reaction (entry 4).

https://doi.org/10.1038/s44160-026-01127-z

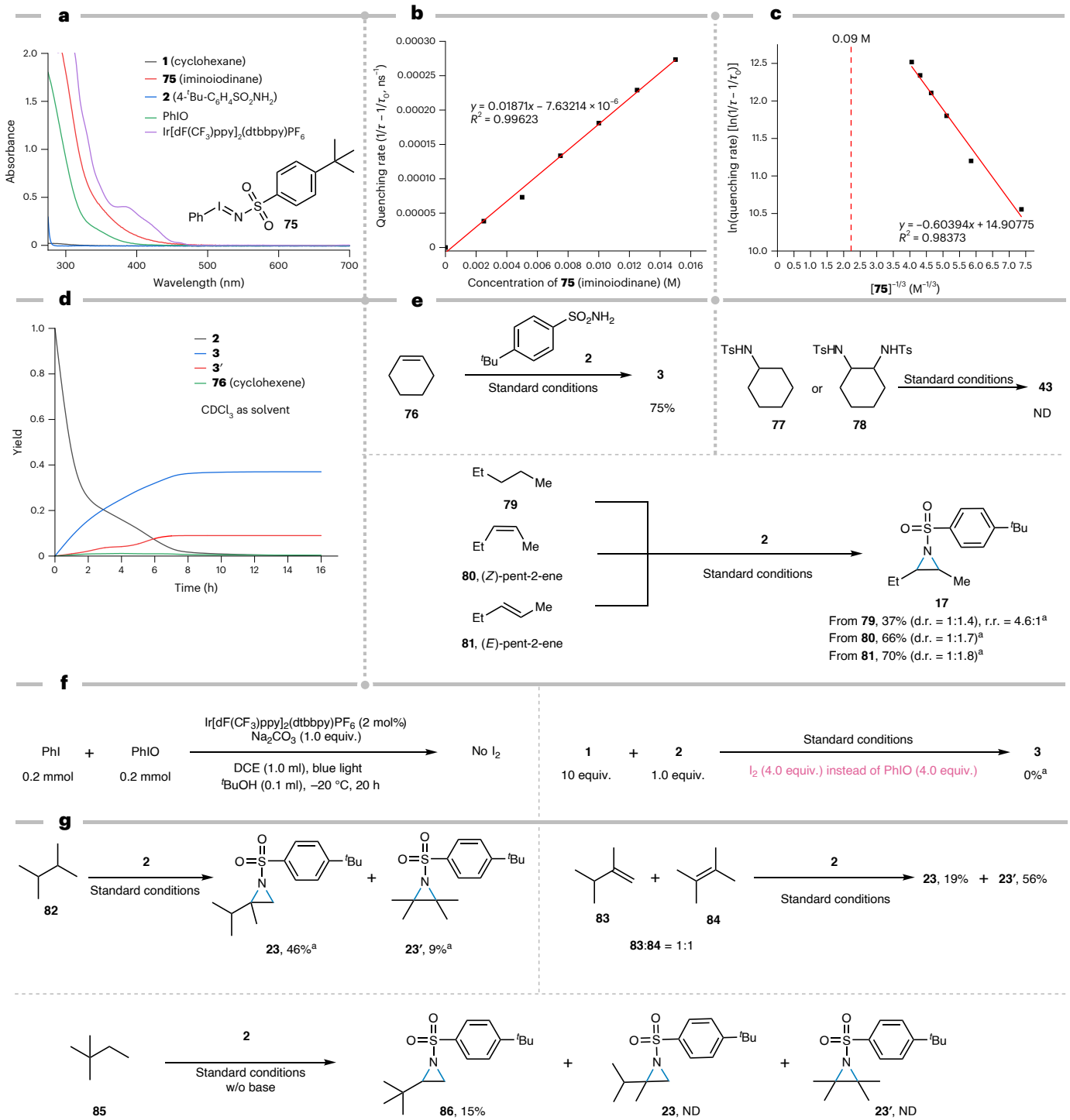

Fig. 4 | Control experiments for mechanistic studies. a, UV–vis absorption spectra. **b**, Pseudolinear plot of the phosphorescence quenching rate ($1/\tau - 1/\tau_0$) versus the concentration of **75**. **c**, Plot of the natural logarithm of the quenching rate as a function of $[\mathbf{75}]^{-1/3}$. The red line shows visual guidance where the Dexter energy transfer mechanism applies (that is, the Dexter regime; ln(quenching rate) $\propto [\mathbf{75}]^{-1/3}$). The vertical red dashed line corresponds to the concentration of **75** employed for the reaction. **d**, Time-course analysis. **e**, Investigation of possible reaction intermediates. **f**, Examination of iodine involvement. **g**, Assessment of cationic species participation. Isolated yields are reported unless otherwise noted. [a]Yields and ratios were based on analysis of the crude ^{1}H NMR spectra.

Increasing the PhIO loading was beneficial for the desired aziridination (entries 5 and 6), whereas alternative hypervalent iodide reagents, such as (diacetoxyiodo)benzene (entry 7), were markedly less effective (Supplementary Table 8). The addition of ^{t}BuOH as a cosolvent improved PhIO solubility, while other solvents proved inferior to the ^{t}BuOH/DCE mixture (Supplementary Table 3). Reaction temperature was crucial for selectivity and yield: raising it above −20 °C decreased the formation of aziridine **3** but increased generation of the amination by-product **3′** (Table 1, entry 8, and Supplementary Table 7). Furthermore, changing the nitrene precursor to a sulfonyl azide resulted in only trace aziridine formation, which could be modestly improved by the addition of PhIO (Table 1, entries 9 and 10, and Supplementary Table 1).

https://doi.org/10.1038/s44160-026-01127-z

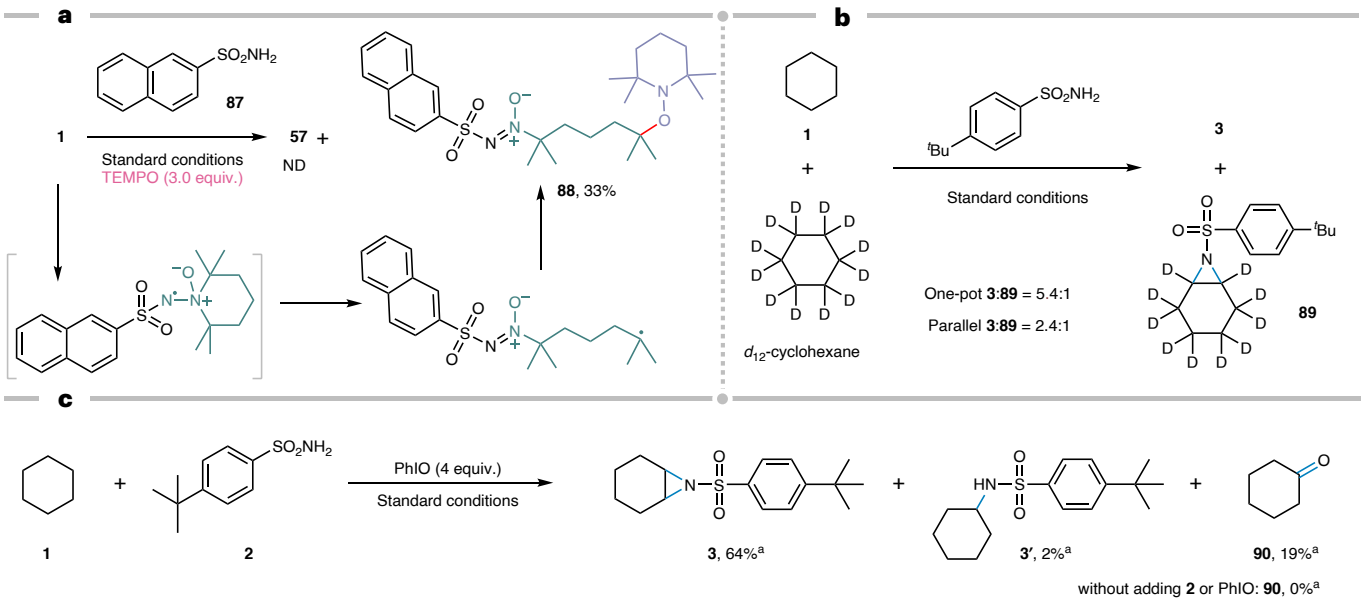

Fig. 5 | Additional control experiments. a, Reaction in the presence of radical scavenger TEMPO. **b**, Exploration of the kinetic isotope effect. **c**, Cyclohexanone formation in the presence of PhIO. Isolated yields are reported unless otherwise noted. [a]Yields and ratios were based on analysis of the crude ^{1}H NMR spectra.

Substrate scope

With the optimized conditions established, we explored the scope of hydrocarbons in the aziridination of vicinal C(sp^3)–H bonds (Fig. 2). A wide variety of cycloalkanes, ranging in size from five to eight carbon atoms, yielded *cis*-aziridine products **4**–**6** exclusively in moderate yields. Larger rings such as cyclododecane produced aziridine **7** as a diastereomeric mixture owing to its less constrained conformation. Fused bicyclic alkanes, such as bicyclo[2.2.1]heptane, were well tolerated, delivering aziridine **8** in 47% yield as a single *exo* isomer. Reactions with indane and tetralin afforded aziridines **9** and **10** in moderate yields. Cycloalkanes with methyl, chlorine or CF_3 substituents also furnished the corresponding aziridines **11**–**14**, albeit with moderate regioselectivities. Remarkably, industrial gaseous alkane feedstocks such as propane and isobutane were successfully converted into the corresponding aziridines **15** and **16** with synthetically useful yields. Furthermore, longer linear aliphatic systems containing multiple hydridic C–H bonds performed well under our standard conditions, favouring reactions at secondary or tertiary C(sp^3)–H bonds (**17**–**20**). For branched alkanes, aziridination preferentially occurred at the statistically abundant terminal vicinal C(sp^3)–H bonds (**21**–**27**). In the case of linear alkanes with electron-withdrawing substituents, such as halogens, ketones, esters, nitriles, phthalimides and sulfones, distal aziridinations (**28**–**36**) were favoured owing to polarity mismatch at the α-C(sp^3)–H bond in the HAT process. Furthermore, hydrocarbons derived from natural products, such as eucalyptol, (−)-fenchone, sclareolide and celestolide, underwent aziridination smoothly to afford products (**37**–**40**) in moderate to good yields with single or acceptable regioselectivities, demonstrating the synthetic utility of our protocol. Notably, while unactivated alkanes exhibited excellent difunctionalization reactivity with negligible C–H amination by-products (less than 5%), activated alkanes, such as ethers, only produced C–H amination at the α-carbon (**41**) without forming aziridine under optimized conditions[26].

Subsequently, we explored the scope of this aziridination with respect to various sulfonamides (Fig. 3a). A wide range of aryl sulfonamides bearing either electron-donating or electron-withdrawing substituents at the *para*-, *meta*- or *ortho*-positions of the aromatic ring readily participated in the aziridination reactions, giving aziridination products (**42**–**54**) in moderate to good yields. Sulfonamides with disubstituted phenyls, sterically bulky naphthyl groups or heteroaromatics (such as thiofuran and pyridine) all underwent successful aziridination with cyclohexane (**55**–**61**). Alkyl-substituted sulfonamides proved viable as well, producing the corresponding aziridines (**62**–**69**) in moderate yields. Furthermore, our protocol is applicable to the late-stage functionalization of aryl sulfonamide-containing pharmaceuticals, such as celecoxib, deracoxib and valdecoxib, enabling aziridination (**70**–**72**) in moderate yields.

To demonstrate the scalability and practical applications of our methodology, we used a simple in-house-built high-speed circulation flow (HSCF) system for large-scale aziridine synthesis[41] (Fig. 3b). This system facilitated decagram-scale photo-mediated aziridinations of cyclohexane **1** or celestolide **73** with 4-*tert*-butylbenzenesulfonamide **2**, yielding aziridines **3** and **40** in moderate yields. The inherent challenges of clogging owing to insoluble Na_2CO_3 and excess PhIO were effectively mitigated by maintaining a high flow rate of 120 ml min^{-1}, enabling the smooth execution of the reaction at −20 °C under 456 nm light irradiation. These results highlight the scalability of our reaction, providing a practical solution for solid-involved transformations using an HSCF system. Notably, the HSCF system was also successfully adapted for the large-scale synthesis of aziridine **16** using isobutane gas **74** with moderate yield, thereby underscoring its versatility and industrial relevance.

Mechanistic studies

To gain a deeper understanding of the mechanistic pathways in the aziridination of alkanes, we conducted a series of experiments aimed at elucidating key steps and intermediates. A light on/off experiment underscores the indispensable role of light in promoting aziridination (Supplementary Fig. 29), while a reaction quantum yield of 0.57% supports a photocatalytic cycle with a non-chain mechanism or a short-lived radical chain process[42] (Supplementary Fig. 28). To elucidate the initiation process of this phototransformation, several spectroscopic measurements were conducted. UV–vis spectra of both the Ir photocatalyst and the in situ-generated iminoiodinane with absorption around 456 nm (Fig. 4a) indicate their activation under the experimental conditions. Phosphorescence decay studies of Ir[dF(CF_3)ppy]$_2$(dtbbpy)PF_6, using time-correlated single-photon-counting techniques, reveal a bimolecular quenching rate constant (k_Q) of 1.87×10^7 M^{-1} s^{-1} obtained through linear regression analysis of

https://doi.org/10.1038/s44160-026-01127-z

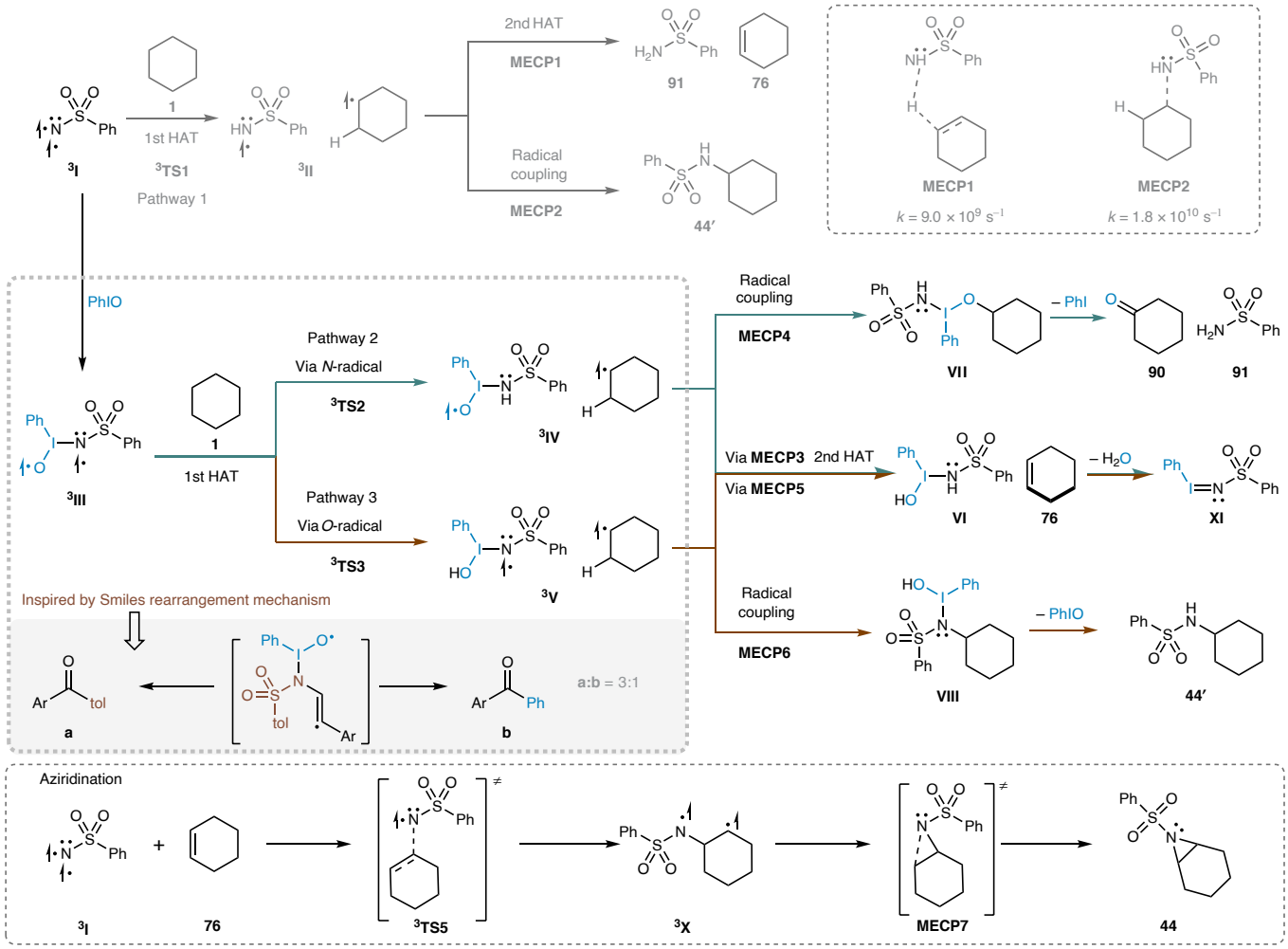

Fig. 6 | Computational studies and proposed mechanisms. Proposed reaction pathways for the double-HAT process and subsequent aziridination based on density functional theory calculations. Pathways 1–3 proceed through triplet nitrene (^{3}**I**) or the nitrene–PhIO adduct (^{3}**III**), followed by sequential HAT steps to generate cyclohexene, which undergoes aziridination via the *N*-centred radical intermediate (^{3}**X**) to afford aziridine **44**. TS, transition state.

the phosphorescence quenching rate versus the concentration of iminoiodinane **75** (Fig. 4b). Further analyses of ln(quenching rate) versus $[\mathbf{75}]^{-1/3}$ and $[\mathbf{75}]^2$ (Fig. 4c and Supplementary Fig. 6, respectively) suggest a predominant Dexter-type energy transfer mechanism across the concentration range studied[43]. In addition, the yields of aziridination products correlated with the triplet energy of the photosensitizers, rather than their redox potential[44] (Supplementary Table 11). Notably, aziridine **3** was still obtained in 28% yield without photocatalysts under 456 nm light irradiation (Table 1, entry 3), consistent with studies by Koenigs and König on the direct generation of triplet sulfonyl nitrenes from excited iminoiodinanes under visible-light irradiation in chlorinated solvents without photosensitizers[24,26]. All these results confirm that triplet nitrene formation is crucial to the reaction, occurring via energy transfer between the excited photosensitizer and iminoiodinane, which was generated in situ from sulfonamides and PhIO[45,46].

With triplet nitrene formation established as a pivotal initial step, we explored additional intermediates to further clarify the progression of the aziridination reaction. Reaction monitoring with ^{1}H NMR spectroscopy in $CDCl_3$ showed complete consumption of sulfonamide **2** within 8 h, accompanied by the formation of the aziridine **3**, by-product **3′** and trace cyclohexene (Fig. 4d). Subjecting cyclohexene to the standard reaction conditions yielded aziridine **3** in high yield, while neither C–H amination by-product **77** nor vicinal diamine **78** produced aziridine (Fig. 4e). Moreover, aziridine **17** obtained from *n*-pentane exhibited diastereoselectivity similar to that from either *E*- or *Z*-pent-2-ene (Fig. 4e), suggesting that alkenes are potential intermediates. A competition experiment demonstrated a markedly faster aziridination rate for alkenes compared with alkanes (Supplementary Fig. 30), highlighting their higher reactivity and crucial mechanistic role, which explains their trace detection in the reaction mixture.

The plausibility of mechanisms involving I_2-mediated radical–polar crossover difunctionalization of alkanes[4,7,47] was ruled out based on experimental evidence. No iodide by-products or I_2 formation was observed when PhI and PhIO were subjected to the standard conditions, and replacing PhIO with I_2 failed to produce any aziridine (Fig. 4f). Moreover, the participation of a carbocation intermediate and a polar elimination pathway was also dismissed (Fig. 4g). Treating 2,3-dimethylbutane **82** under standard conditions resulted in terminal aziridine **23** as the major isomer, contradicting the expectation of carbocation pathways that would favour isomer **23′** owing to the thermodynamic stability of tetramethylethylene **84**. This finding is further substantiated by the aziridination of 2,2-dimethylbutane **85**, which exclusively produced aziridine **86** without cation rearrangement to form products **23** or **23′**. The involvement of a radical pathway with triplet nitrene was confirmed by reaction inhibition with the radical scavenger (2,2,6,6-tetramethylpiperidin-1-yl)oxyl (TEMPO), and the isolation of TEMPO adduct **88**, with its structure elucidated

https://doi.org/10.1038/s44160-026-01127-z

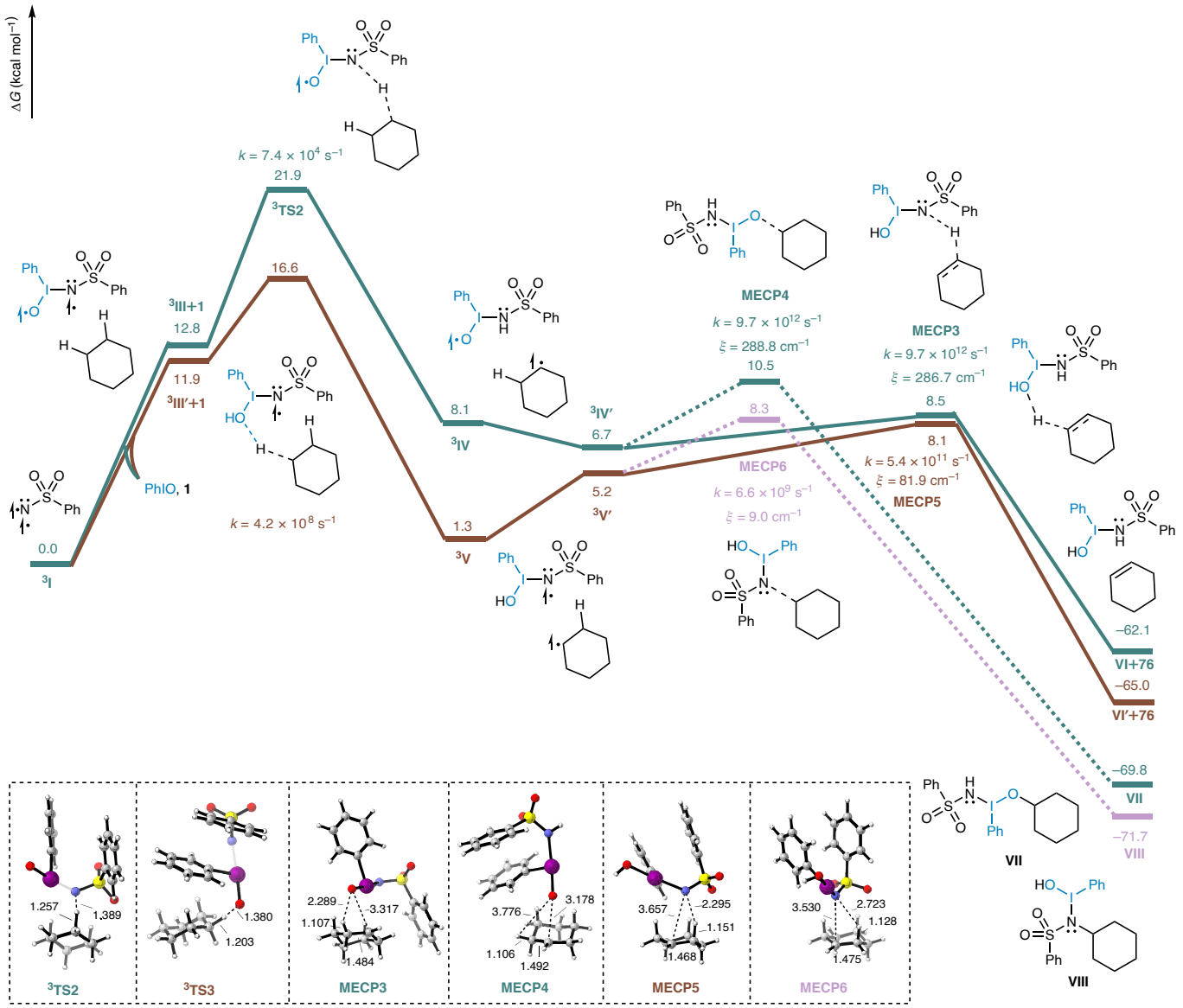

Fig. 7 | Potential energy profiles for the double-HAT process. Energy profiles for triplet sulfonyl nitrene/PhIO-mediated double-HAT pathways at the ωB97XD/def2-TZVPP//def2-SVP/SMD(DCE) level of theory. The reported energies are Gibbs free energies calculated at 253.15 K (−20 °C) and 1 M standard concentration.

by X-ray crystallography, showing two TEMPO molecules trapped by one sulfonyl nitrene intermediate (Fig. 5a). Deuterium labelling studies conducted using cyclohexane and d_{12}-cyclohexane with sulfonamide **2** in either a single vessel or separate vessels yielded k_H/k_D values of 5.4 and 2.4, respectively (Fig. 5b), suggesting that C–H cleavage is involved in the rate-determining step.

Computational studies

Density functional theory calculations were performed to gain deeper mechanistic insights, beginning with the hypothesis that triplet nitrene ^{3}**I** could sequentially abstract two hydrogen atoms from cyclohexane, forming a cyclohexene intermediate while regenerating sulfonamide **91** (Fig. 6, Pathway 1). Unlike typical adiabatic processes, the second HAT step involves a nonadiabatic, spin-forbidden transition from an open-shell triplet to a closed-shell ground state, such that both the minimum energy crossing point (MECP) energy between the two spin states and the magnitude of spin–orbit coupling (ζ) are critical in governing reaction kinetics, rather than the MECP energy or a conventional transition state alone. Accordingly, our analysis incorporates both transition state theory[48] and Marcus theory[49] to assess the feasibility of this second HAT process[49,50]. For Pathway 1, the calculations indicated that intermediate ^{3}**II**, generated after the initial HAT ($k = 2.3 \times 10^7$ s^{-1}, Supplementary Table 16), can undergo either radical coupling to yield by-product **44′** ($k = 1.8 \times 10^{10}$ s^{-1}) or a second HAT step ($k = 9.0 \times 10^9$ s^{-1}, Supplementary Fig. 45). Even after accounting for the statistical factor of four equivalent C–H bonds, the second HAT step ($k = 3.6 \times 10^{10}$ s^{-1}) remains kinetically competitive with radical coupling. However, this picture does not fully align with the experimental observations, which showed only trace amounts of **44′** (<5% yield). In addition, using sulfonyl azide as the nitrene precursor produced less than 0.5% aziridine (Table 1, entry 9), suggesting that ^{3}**I** alone is insufficient to drive the double-HAT process under the reaction conditions. Control experiments further revealed that the formation of both aziridine and cyclohexanone by-product **90** increased with increasing PhIO equivalents (Table 1 and Fig. 5c), indicating a crucial role for PhIO in the reaction mechanism. Further experiments excluded the possibility of PhIO acting as a Lewis acid[51] (Supplementary Table 10). Taken together, these results suggest that although Pathway 1 is accessible according to our computations, PhIO-assisted pathways are more consistent with the experimental observations.

We then investigated two additional mechanistic pathways (Fig. 6, Pathways 2 and 3) involving a diradical nitrene–PhIO adduct intermediate (^{3}**III**). Although challenging to detect, evidence supporting this adduct arises from a separate study on nitrene-promoted Smiles rearrangement under similar conditions, in which replacing alkane substrates with aryl alkynes yielded the predicted ketone product along with a minor PhIO-derived by-product (Supplementary Fig. 31). Pathway 2 involves the first HAT from an N-centred radical with a calculated rate constant of $7.4 \times 10^4\ s^{-1}$ (^{3}**TS2**, transition state theory), followed by a second HAT from the *O*-centred radical with a rate constant of $9.7 \times 10^{12}\ s^{-1}$ (**MECP3**, Marcus theory) (Fig. 7; see Supplementary Section 9 for more computational details). This sequence leads to cyclohexene, which rapidly undergoes aziridination, a well-documented and energetically favourable transformation with triplet nitrenes (Supplementary Fig. 46). While C–O coupling by-product **VII**, en route to cyclohexanone, can also form with a rate constant comparable to that of the second HAT ($k = 9.7 \times 10^{12}\ s^{-1}$, **MECP4**), this off-pathway process regenerates sulfonamide and therefore is not expected to diminish the yield of aziridination, while still providing a plausible origin for the trace cyclohexanone observed experimentally. Alternatively, Pathway 3 involves a first HAT from the *O*-radical with a rate constant of $4.2 \times 10^8\ s^{-1}$ (^{3}**TS3**), followed by a second HAT from the *N*-radical with a rate around $5.4 \times 10^{11}\ s^{-1}$ (**MECP5**). The competing C–N radical coupling step proceeds with a calculated rate constant of around $6.6 \times 10^9\ s^{-1}$ (**MECP6**), approximately two orders of magnitude slower than the second HAT owing to the much larger spin–orbit coupling matrix element for the HAT step, indicating that the second HAT is kinetically favoured over coupling.

Importantly, by further accounting for the reactant preassociation process, the apparent rate constants for the first HAT step in Pathways 1–3 are estimated to be on the order of 10^{-1}, 10^{-7} and $10^{-2}\ s^{-1}$, respectively (Fig. 6 and Supplementary Fig. 45). These values serve as conservative lower bounds for the kinetic competency of each pathway. Across all three pathways, the first HAT process is calculated to be rate-determining, and the final product distribution is governed by competition between the second HAT step and subsequent radical coupling processes. The calculations indicate that Pathway 1 is kinetically feasible, but they do not by themselves establish the relative contributions of Pathways 1–3 under the experimental conditions. Experimentally, however, the strong dependence of both aziridine and cyclohexanone formation on the presence of PhIO, together with the negligible aziridination observed in the absence of PhIO, supports the involvement of PhIO-assisted pathways in the productive reaction manifold. Within this framework, Pathway 2 provides a plausible rationale for the trace formation of the cyclohexanone by-product, whereas Pathway 3 offers the best overall agreement with the observed predominance of aziridine formation. We therefore consider Pathway 3 to be the most reasonable working model at this stage, while Pathways 1 and 2 remain feasible minor routes. Notably, the high energy required for singlet nitrene insertion into alkane C–H bonds suggests that it is not a competitive background reaction (Supplementary Fig. 45). Lastly, aziridination of alkenes proceeds via a well-documented mechanism[24]: addition of the triplet sulfonyl nitrene to cyclohexene **76** generates the *N*-centred radical intermediate ^{3}**X**, which then undergoes intramolecular radical recombination through **MECP7** to furnish aziridine **44** (Fig. 6).

Conclusion

In summary, we have found that the diradical nature of photo-generated triplet sulfonyl nitrenes facilitates a distinctive double-HAT process in the presence of PhIO, enabling direct aziridination of unactivated alkanes. The synthetic potential of this methodology was exemplified by the successful aziridination of a variety of unactivated alkanes, including feedstock gaseous alkanes such as propane and isobutane, late-stage functionalization of natural products and scalable decagram-level synthesis using an HSCF system. Mechanistic investigations indicate the involvement of an alkene intermediate, rather than cationic or iodine-based species, in the reaction pathway. Computational studies further emphasize the critical role of the triplet sulfonyl nitrene together with PhIO in orchestrating the double-HAT process. This work highlights the potential of leveraging diradical or diradical-like intermediates to expand the toolbox for dual C–H functionalization via double-HAT pathways.

Methods

Typical photochemical aziridination procedure for unactivated alkanes

To a Schlenk tube were added $Ir[dF(CF_3)ppy]_2(dtbbpy)PF_6$ (2.2 mg, 0.002 mmol, 0.02 equiv.), PhIO (88.0 mg, 0.40 mmol, 4.0 equiv.), Na_2CO_3 (10.6 mg, 0.10 mmol, 1.0 equiv.) and RSO_2NH_2 (0.10 mmol, 1.0 equiv.). The tube was evacuated and back-filled with argon (repeated three times), followed by the addition of ^{t}BuOH (0.1 ml), alkane (1.0 mmol, 10.0 equiv.) and DCE (1.0 ml). The tube was then sealed and exposed to a blue light-emitting diode (LED) (20 W, maximum 40 W, adjusted to 50%, 456 nm, positioned 2–3 cm away) at −20 °C with stirring (owing to the presence of multiple solids, a rotation speed greater than 800 rpm was necessary to maintain productivity). The reaction was stirred until thin-layer chromatography analysis indicated complete consumption of the sulfonamide (typically 20 h). The reaction mixture was then diluted with dichloromethane (5.0 ml), filtered, and the filtrate was washed with additional dichloromethane (2 × 5.0 ml). The combined organic phases were concentrated under vacuum, and the residue was purified by column chromatography to yield the desired aziridine product.

Data availability

Details about the materials and methods, experimental procedures, mechanistic studies, characterization data, crystallographic data and NMR spectra are available in Supplementary Information. The authors declare that all other data supporting the findings of this study are available within the article and Supplementary Information files. Crystallographic data for the structures reported in this article have been deposited at the Cambridge Crystallographic Data Centre, under deposition number CCDC 2422923 (**88**). Copies of the data can be obtained free of charge via https://www.ccdc.cam.ac.uk/structures/.

References

1. Yu, J.-Q. & Shi, Z. *C–H Activation*. *Topics in Current Chemistry* Vol. 292 (Springer, 2010).
2. Cao, H., Tang, X., Tang, H., Yuan, Y. & Wu, J. Photoinduced intermolecular hydrogen atom transfer reactions in organic synthesis. *Chem. Catal.* **1**, 523–598 (2021).
3. Capaldo, L., Ravelli, D. & Fagnoni, M. Direct photocatalyzed hydrogen atom transfer (HAT) for aliphatic C–H bonds elaboration. *Chem. Rev.* **122**, 1875–1924 (2022).
4. Barluenga, J., González-Bobes, F. & González, J. M. Activation of alkanes upon reaction with $PhI(OAc)_2$–I_2. *Angew. Chem. Int. Ed.* **41**, 2556–2558 (2002).
5. Shen, T., Li, Y.-L., Ye, K.-Y. & Lambert, T. H. Electrophotocatalytic oxygenation of multiple adjacent C–H bonds. *Nature* **614**, 275–280 (2023).
6. Kundu, G. & Lambert, T. H. Electrochemical vicinal C–H difunctionalization of saturated azaheterocycles. *J. Am. Chem. Soc.* **146**, 1794–1798 (2024).
7. Prusinowski, A. F., Twumasi, R. K., Wappes, E. A. & Nagib, D. A. Vicinal double C–H functionalization of alcohols via an imidate radical–polar crossover cascade. *J. Am. Chem. Soc.* **142**, 5429–5438 (2020).
8. Shen, T. & Lambert, T. H. Electrophotocatalytic diamination of vicinal C–H bonds. *Science* **371**, 620–626 (2021).

9. Huang, L., Bismuto, A., Rath, S. A., Trapp, N. & Morandi, B. Ruthenium-catalyzed dehydrogenation through an intermolecular hydrogen atom transfer mechanism. *Angew. Chem. Int. Ed.* **60**, 7290–7296 (2021).
10. Voica, A.-F., Mendoza, A., Gutekunst, W. R., Fraga, J. O. & Baran, P. S. Guided desaturation of unactivated aliphatics. *Nat. Chem.* **4**, 629–635 (2012).
11. Zhou, M.-J., Zhang, L., Liu, G., Xu, C. & Huang, Z. Site-selective acceptorless dehydrogenation of aliphatics enabled by organophotoredox/cobalt dual catalysis. *J. Am. Chem. Soc.* **143**, 16470–16485 (2021).
12. Novaes, L. F. T. et al. α,β-Desaturation and formal β-C(sp^3)–H fluorination of *N*-substituted amines: a late-stage functionalization strategy enabled by electrochemistry. *J. Am. Chem. Soc.* **146**, 22982–22992 (2024).
13. Vedernikov, A. N. & Caulton, K. G. Facile alkane functionalization in copper-[2.1.1]-(2,6)-pyridinophane-PhINTs systems. *Chem. Commun.* **2004**, 162–163 (2004).
14. Breslow, R. et al. Remote oxidation of steroids by photolysis of attached benzophenone groups. *J. Am. Chem. Soc.* **95**, 3251–3262 (1973).
15. Conde, A. et al. Introducing copper as catalyst for oxidative alkane dehydrogenation. *J. Am. Chem. Soc.* **135**, 3887–3896 (2013).
16. West, J. G., Huang, D. & Sorensen, E. J. Acceptorless dehydrogenation of small molecules through cooperative base metal catalysis. *Nat. Commun.* **6**, 10093 (2015).
17. Jagtap, R. A. et al. Catalytic acceptorless complete dehydrogenation of cycloalkanes. *Nat. Commun.* **16**, 428 (2025).
18. Zhou, S., Zhang, Z.-J. & Yu, J.-Q. Copper-catalysed dehydrogenation or lactonization of C(sp^3)–H bonds. *Nature* **629**, 363–369 (2024).
19. Gu, X. et al. Synthesis of non-canonical amino acids through dehydrogenative tailoring. *Nature* **634**, 352–358 (2024).
20. Niu, D., Willoughby, P. H., Woods, B. P., Baire, B. & Hoye, T. R. Alkane desaturation by concerted double hydrogen atom transfer to benzyne. *Nature* **501**, 531–534 (2013).
21. Wang, Y.-C. et al. Unravelling nitrene chemistry from acyclic precursors: recent advances and challenges. *Org. Chem. Front.* **8**, 1677–1693 (2021).
22. Dequirez, G., Pons, V. & Dauban, P. Nitrene chemistry in organic synthesis: still in its infancy? *Angew. Chem. Int. Ed.* **51**, 7384–7395 (2012).
23. Narobe, R. & König, B. Transformations based on direct excitation of hypervalent iodine(III) reagents. *Org. Chem. Front.* **10**, 1577–1586 (2023).
24. Guo, Y., Pei, C. & Koenigs, R. M. A combined experimental and theoretical study on the reactivity of nitrenes and nitrene radical anions. *Nat. Commun.* **13**, 86 (2022).
25. Guo, Y., Pei, C., Empel, C., Jana, S. & Koenigs, R. M. Photochemical nitrene transfer reactions of iminoiodinanes with sulfides. *ChemPhotoChem* **6**, e202100293 (2022).
26. Jurberg, I. D., Nome, R. A., Crespi, S., Atvars, T. D. Z. & König, B. Visible light-enhanced C–H amination of cyclic ethers with iminoiodinanes. *Adv. Synth. Catal.* **364**, 4061–4068 (2022).
27. Li, F. et al. Photosensitization enables Pauson–Khand-type reactions with nitrenes. *Science* **383**, 498–503 (2024).
28. Gibian, M. J. & Corley, R. C. Organic radical–radical reactions. Disproportionation vs. combination. *Chem. Rev.* **73**, 441–464 (1973).
29. Florio, S. & Luisi, R. Aziridinyl anions: generation, reactivity, and use in modern synthetic chemistry. *Chem. Rev.* **110**, 5128–5157 (2010).
30. Stanković, S. et al. Regioselectivity in the ring opening of non-activated aziridines. *Chem. Soc. Rev.* **41**, 643–665 (2012).
31. Biswas, P., Maity, A., Figgins, M. T. & Powers, D. C. Aziridine group transfer via transient *N*-aziridinyl radicals. *J. Am. Chem. Soc.* **146**, 30796–30801 (2024).
32. Müller, P. & Fruit, C. Enantioselective catalytic aziridinations and asymmetric nitrene insertions into C–H bonds. *Chem. Rev.* **103**, 2905–2920 (2003).
33. Jat, J. L. et al. Direct stereospecific synthesis of unprotected N–H and N–Me aziridines from olefins. *Science* **343**, 61–65 (2014).
34. Mitchell, J. K., Hussain, W. A., Bansode, A. H., O'Connor, R. M. & Parasram, M. Aziridination via nitrogen-atom transfer to olefins from photoexcited azoxy-triazenes. *J. Am. Chem. Soc.* **146**, 9499–9505 (2024).
35. Cheng, Q.-Q. et al. Organocatalytic nitrogen transfer to unactivated olefins via transient oxaziridines. *Nat. Catal.* **3**, 386–392 (2020).
36. Ošeka, M. et al. Electrochemical aziridination of internal alkenes with primary amines. *Chem* **7**, 255–266 (2021).
37. Holst, D. E., Wang, D. J., Kim, M., Guzei, I. A. & Wickens, Z. K. Aziridine synthesis by coupling amines and alkenes via an electrogenerated dication. *Nature* **596**, 74–79 (2021).
38. Tan, H. et al. Metal-free aziridination of unactivated olefins via transient *N*-pyridinium iminoiodinanes. *JACS Au* **4**, 4187–4193 (2024).
39. Brägger, Y. et al. Oxidative amination by nitrogen atom insertion into carbon–carbon double bonds. *Science* **387**, 1108–1114 (2025).
40. Gelato, Y. et al. Iodonitrene-mediated nitrogen transfer to alkenes for the direct synthesis of NH-aziridines. *J. Am. Chem. Soc.* **147**, 35567–35575 (2025).
41. Liu, C. et al. High-speed circulation flow platform facilitating practical large-scale heterogeneous photocatalysis. *Org. Process Res. Dev.* **28**, 1964–1970 (2024).
42. Cismesia, M. A. & Yoon, T. P. Characterizing chain processes in visible light photoredox catalysis. *Chem. Sci.* **6**, 5426–5434 (2015).
43. Soni, V. K. et al. Generation of *N*-centered radicals via a photocatalytic energy transfer: remote double functionalization of arenes facilitated by singlet oxygen. *J. Am. Chem. Soc.* **141**, 10538–10545 (2019).
44. Strieth-Kalthoff, F., James, M. J., Teders, M., Pitzer, L. & Glorius, F. Energy transfer catalysis mediated by visible light: principles, applications, directions. *Chem. Soc. Rev.* **47**, 7190–7202 (2018).
45. Alderson, J. M., Phelps, A. M., Scamp, R. J., Dolan, N. & Schomaker, J. M. Ligand-controlled, tunable silver-catalyzed C–H amination. *J. Am. Chem. Soc.* **136**, 16720–16723 (2014).
46. Dolan, N. S., Scamp, R. J., Yang, T., Berry, J. F. & Schomaker, J. M. Catalyst-controlled and tunable, chemoselective silver-catalyzed intermolecular nitrene transfer: experimental and computational studies. *J. Am. Chem. Soc.* **138**, 14658–14667 (2016).
47. Bering, L. & Antonchick, A. P. Selective transition-metal-free vicinal *cis*-dihydroxylation of saturated hydrocarbons. *Chem. Sci.* **8**, 452–457 (2017).
48. Eyring, H. The activated complex in chemical reactions. *J. Chem. Phys.* **3**, 107–115 (1935).
49. Marcus, R. A. On the theory of electron-transfer reactions. VI. Unified treatment for homogeneous and electrode reactions. *J. Chem. Phys.* **43**, 679–701 (1965).
50. Yarkony, D. R. Diabolical conical intersections. *Rev. Mod. Phys.* **68**, 985–1013 (1996).
51. Macikenas, D., Skrzypczak-Jankun, E. & Protasiewicz, J. D. Redirecting secondary bonds to control molecular and crystal properties of an iodosyl- and an iodylbenzene. *Angew. Chem. Int. Ed.* **39**, 2007–2010 (2000).

Acknowledgements
J.W., H.T.A. and C.W. thank computation resources from NUS IT's Research Computing group under NUSREC-HPC-00001. K.N.H. and Q.-Y.Z. thank computation resources from Expanse at SDSC through allocation CHE040014 from the Advanced Cyberinfrastructure Coordination Ecosystem: Services & Support (ACCESS) programme. J.W. thanks Z. Dong (SUSTech) for insightful discussion.

Author contributions
M.-S.L. and J.W. conceived of and designed the research. J.W. guided the project. M.-S.L. performed the experiments. M.-S.L., J.-L.A. and Z.-H.J. prepared the starting materials. M.-S.L., H.T.A., C.W., X.-Y.Y., J.-L.A. and J.W. analysed the data. H.T.A., Q.-Y.Z., C.W. and K.N.H. performed the density functional theory calculations. M.-S.L., H.T.A., C.W., G.W., K.N.H. and J.W. wrote the paper. All authors gave approval to the final version of the paper.

Funding
J.W. discloses support for the research of this work from the National Research Foundation, the Prime Minister's Office of Singapore, under its NRF-CRP Programme (NRFCRP25-2020RS-0002), the SUSTech-NUS Joint Research Program, Ministry of Education of Singapore (T2EP10224-0005). K.N.H. discloses support for publication of this work from the National Science Foundation (CHE-2153972).

Competing interests
The authors declare no competing interests.

Additional information
Supplementary information The online version contains supplementary material available at https://doi.org/10.1038/s44160-026-01127-z.

Correspondence and requests for materials should be addressed to Kendall N. Houk or Jie Wu.

Peer review information *Nature Synthesis* thanks Joshua Barham and the other, anonymous, reviewer(s) for their contribution to the peer review of this work. Primary Handling Editor: Thomas West, in collaboration with the *Nature Synthesis* team.